

Effects Of the Length and Location Heat Source on The Assisting Mixed Convection in A Channel Attached to Parallelogram Cavity

Amal Abdul Razaq Abdul Hussein^{1*}, Ahmed Kadhim Hussein²

^{1,2*} Mechanical Engineering Department, University of Babylon, Iraq.

E-mail: amal.hussein@student.uobabylon.edu.iq

Abstracts: The current research presents a numerical investigate of the effect of the heat source length and location on the mixed convection aiding flow inside the horizontal channel attached with an open parallelogram cavity .When the heated wall is on the same side of the force inflow .The heat source length was considered as (ϵ) ($0.25 < \epsilon < 1$) with a different in the location of the heat source on sidewalls of the cavity. The cold airflow and fixed velocity enter the channel horizontally. The vertical walls in the inflow and outflow sides are isothermal while all other walls are adiabatic. The flow and thermal fields computed for a wide range of Richardson numbers ($Ri=0.1-100$) While, both Reynolds and Prandtl numbers are kept constant at ($Re = 100$) and ($Pr = 0.71$). The results were presented of the flow and thermal fields, average Nusselt numbers. The results show that a rate of heat transfer is increase with in increasing in Richardson numbers (Ri) and the length of the heat source(ϵ). Also, it was found that, the maximum average Nusselt number is achieved in the upper region of the right wall of the cavity for all values of Richardson number.

Keywords: Aiding mixed convection, Parallelogram cavity, Horizontal channel.

1. INTRODUCTION

Due to the widespread applications of the mixed convection (or combined convection) in a variety of industrial and technological operations .Heat exchangers for cooling and heating fluid, compact heat exchangers, furnaces, nuclear reactors, and the food industry are just a few example [1-4]; hence, over the recent years the mixed convection in cavities received a clear attention because of their apps like float glass processing ,composite materials manufacturing , electronic chips ,cooling of electronic devices ,ingot quenching, energy extraction, polymer crystallization [5- 13]. In this context, **Manca et al. [14]**, present a numerically study of the combined convection inside a channel with a U-shaped open cavity. The cold airflow entered the channel with a constant heat flux at three different heating modes were considered (i.e., opposing flow ,assisting flow , and heating from below, while the other walls were kept adiabatic. They concluded that, when the (Re) and (Ri) numbers increased, the maximum temperature decreased. Later, **Manca et al. [15]** , investigated experimentally the laminar mixed convection . A cold air was introduced he channel from the left sidewall at uniform velocity. All the channel and cavity walls are assumed thermally insulated except the left side wall is heated at uniform heat flux. It was found that, the (Nu_{av}) increasing with increasing the aspect ratio of the cavity for all consider range of (Re) and(Ri) numbers. **Leong et al. [16]**, a numerically studied of the combined convection inside the channel with a cavity heated from below. They concluded that, the flow field was controlled by (Gr). and (Re). **Aminossadati and Ghasemi [17]**. carried out a numerical study of the combined convection in horizontal channel and connected with an open cavity below it. The case study is done for a mixed convection air entered the channel integration with an open rectangular cavity with a discrete heat source located on three different locations (left, right and bottom walls) .It was found that, the heat transmission was improved when the cavity aspect ratio increased of the cavity for three different locations of the heat source and fixed value of (Ri) number. **Rahman et al. [18]**, studied numerically the combined convection in a horizontal channel with a rectangular cavity heated from below. A magnetic field was subjected to the channel-cavity assembly from its right side. They deduced that, the (Nu_{av}) was increase by increasing the (Re) and (Ra) numbers and it was decrease by increasing the (Ha)number. The numerical investigation of the combined free-forced convection in a horizontal channel with an open rectangular cavity by **Rahman et al. [19]**. The rectangular cavity included at its center a hollow cylinder which was heated from its inner side by a uniform heat flux. It was found that, the (Nu_{av}) at the heated surface enhanced as (Ra) number and thermal conductivities increased and was static with increasing in (Pr). **Carozza et al. [20]** analyzed numerically the combined convection in a square cavity with a forced air flow entered from the channel located above it. The left and right-side walls of the cavity were maintained at a hot and cold temperature was respectively. Two cases were considered (assisting flow, opposing flow). They came to the conclusion that raising (Re) raised the (Nu_{av}) in both

cases. **Laouira et al. [21]**, investigated numerically the effects of the length of the heat source on the combined convection in a duct with an open trapezoidal enclosure which the base of enclosure was heated by a discrete heat source. It was found, the (Nu_{av}) increased with increasing in (ϵ) . **Mebarek- Oudina et al. [22]**, present a numerical simulation of the laminar combined convection of air in a horizontal channel with an open trapezoidal enclosure locational below it. The walls of the enclosure was subjected to a localized hot source of a finite length insulated. They came to the conclusion that heat transfer reached its peak value when the heat source was placed in the top of the left wall. **Al- Farhany et al. [23]**, investigated numerically the combined convection inside the channel with an open complex enclosure and subjected a discrete heated source at its bottom wall channel. a magnetic field was subjected to the channel–cavity assembly from its right side while, the air was entered the channel from its left side. They deduced that, the (Nu_{av}) as increased with the increase of (Ri) and decreases of (Ha) .

Further works about the combined convection in an open cavity attached with a channel can be found in [23-35]. In this paper, the effects of heat source length and its location on the combined convection in a channel attach with a parallelogram cavity. Air was introduced to the channel at a uniform velocity and a cold temperature. The effect of the heated wall location and length on the mixed convection of air with a wide range of Richardson number were investigated numerically. The numerical results are presented in the form of the velocity, isotherms contours and Nusselt numbers profiles, while the (Re) and (Pr) were fixed respectively at 100 and 0.71.

2. GEOMETRY DESCRIPTION AND THE GOVERNING EQUATIONS

The geometry under studied is shown in Figure (1). The channel of diameter (D) combined with an open cavity. The free length of the channel beyond the cavity (L_e) is equal to $(1H)$. The height of the cavity is (W) and length $(L=2H)$ is illustrated. Air flow enters the channel horizontally from its left side at uniform velocity (u_{in}) with a cold temperature (T_c) . The length of heat source is (L_H) was at a hot temperature (T_h) at the left sidewall of the cavity by using discrete heat sources at a two different location of heat source (the center of the left wall and the upper region of the same wall with a different length of heat source, while the other walls are assumed adiabatic. The simplifying assumptions used for this study:

1. Steady, incompressible, two-dimensional, Newtonian and laminar flow.
2. Radiation and heat generation are neglected.
3. The thermo-physical characteristics of the air were kept fixed. Furthermore, the Boussinesq approximation was adopted to solve the dependency of the density-temperature

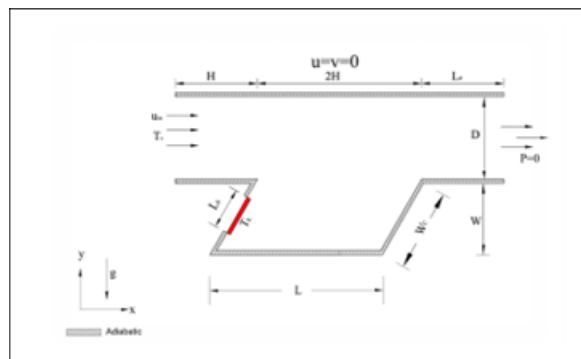


Figure 1. Geometry of the problem.

In Cartesian coordinates, the dimensionless form of the governing equations in the present work which are given as [15,18]

$$\frac{6U}{6K} + \frac{6V}{6F} = 0 \tag{1}$$

$$U \frac{\partial U}{\partial X} + V \frac{\partial U}{\partial Y} = -\frac{\partial P}{\partial X} + \frac{1}{Re_{in}} \left(\frac{\partial^2 U}{\partial X^2} + \frac{\partial^2 U}{\partial Y^2} \right), \tag{2}$$

$$U \frac{\partial V}{\partial X} + V \frac{\partial V}{\partial Y} = -\frac{\partial P}{\partial Y} + \frac{1}{Re_{in}} \left(\frac{\partial^2 V}{\partial X^2} + \frac{\partial^2 V}{\partial Y^2} \right) + Ri\theta, \tag{3}$$

$$U \frac{\partial \theta}{\partial X} + V \frac{\partial \theta}{\partial Y} = \frac{1}{Re_{in} Pr} \left(\frac{\partial^2 \theta}{\partial X^2} + \frac{\partial^2 \theta}{\partial Y^2} \right), \tag{4}$$

Where:

It is worth to mention that the Richardson number represents the ratio between the free convection and the forced convection. In the present study, the free convection effect is due to the buoyancy force generated by the cold and the hot temperature. However, the forced convection term included in the Richardson number is due to the channel flow. The boundary conditions are given by;

$$X, Y = \frac{x, y}{W}, \quad U, V = \frac{u, v}{u_{in}}, \quad \theta = \frac{T - T_c}{T_h - T_c}, \quad P = \frac{p}{\rho u_{in}}, \quad Pr = \frac{\nu}{\alpha}, \quad Re_{in} = \frac{\rho u_{in} W}{\mu}, \quad \varepsilon = \frac{L_H}{W}$$

$$Ri = \frac{Gr}{Re_{in}^2} = \frac{gW\beta(T_h - T_c)}{u_{in}^2} \tag{5}$$

Channel entrance: $X=0 \quad H \leq Y \leq W+D \quad \theta=1, \quad u_{in}=1$ (6)

Channel exit: $X=4H \quad H \leq Y \leq W+D, \quad \frac{6\theta}{6K} = 0, \quad \frac{6U}{6K} = \frac{6V}{6F} = 0, \quad P=0$ (7)

On the heater: $\theta=1$, otherwise, $0n \cdot \left(\frac{6\theta}{6n} \right) = 0$, where (n) is the normal vector.

On no slip boundary condition is applied to the solid stationary walls: $U = V = 0$. (8)

The flow field inside the channel-enclosure assembly can be characterized by using the dimensionless stream function (Ψ) which can be obtained from the dimensionless velocity components (U and V) as follows:

$$U = \frac{6V}{6F} \quad \text{and} \quad V = -\frac{6U}{6K} \tag{9}$$

Where $T = \frac{f}{\alpha}$; Hence, by using Eq. (9) with the continuity equation (Eq. (1)), we get the following Poisson's equation:

$$\frac{\partial^2 T}{\partial X^2} + \frac{\partial^2 T}{\partial Y^2} = \frac{\partial U}{\partial Y} - \frac{\partial V}{\partial X} \tag{10}$$

Once U and V are found, Eq. (10) is solved numerically with the appropriate boundary conditions to find Ψ . The average Nusselt number can be computed by integrating the local temperature gradient at the hot source and can be represented by

$$Nu_{av} = \frac{1}{L_h} \int_0^{L_h} \theta \, dY \tag{11}$$

Where L_h is the heat source length (ϵ)

3. VALIDATION AND GRID INDEPENDENCY ANALYSIS

During the current research, the COMSOL software was used to compute the numerical results. The first challenge is to convert the partial differential equations (i.e., Eqs. (1)-(4)) with their related boundary conditions in to linear algebraic equations to solve them easily. The physical domain of the problem is discretized into several elements linked by nodes and represented by algebraic linear equations. The residuals of each conservation equation are computed by substituting the approximations into the Navier stokes equations. To select the suitable grid size, which is required to reduce the time of the computation, the first step is to check the grid-independency. This test was performed by using six different elements numbers for each heat source depending on the different average Nusselt number. Six grid sizes were tested at (Ri=0.1,1,10,100, Pr =0.7 and Re = 100) (see Table 1). It was found that the values of the Nu_{avg} for G6 (44316 elements) grid is almost identical with a very small error (< 0.9 %). Therefore, a grid size of G6 (44316 elements) is selected in the numerical solution due to its time-economy merit and small deviations in the average Nusselt number. In order to check the current work results, **Manca et al. [15]** case is re-solved by the present model as it presented in Fig.2 and a good concordance between the two results is observed.

Table 1. Variation of the average Nusselt number Nu_{avg} for various grids for assigns flow frombelow at (Pr =0.7, $\epsilon = 1$, Ri = 0.1, 1, 10,100 and Re=100).

	Ri							
	Ri=0.1	[Error%]	Ri=1	[Error%]	Ri=10	[Error%]	Ri=100	[Error%]
G1(1928)	2.4178	—	3.2635	—	5.1522	—	8.9287	—
G2(2988)	2.4279	0.416	3.2671	0.1102	5.0953	1.1044	8.4527	5.332
G3(4852)	2.4349	0.2875	3.2719	0.1467	5.0684	0.528	8.1844	3.1742
G4(11680)	2.4586	0.964	3.2981	0.7944	5.0845	0.31665	8.1302	0.663
G5(28634)	2.47207	0.5448	3.3119	0.41668	5.0955	0.21587	8.0517	0.965
G6(44316)	2.4702	0.0756	3.3113	0.01812	5.0916	0.0765	7.9805	0.884
Manca et al. [15]					Present work			

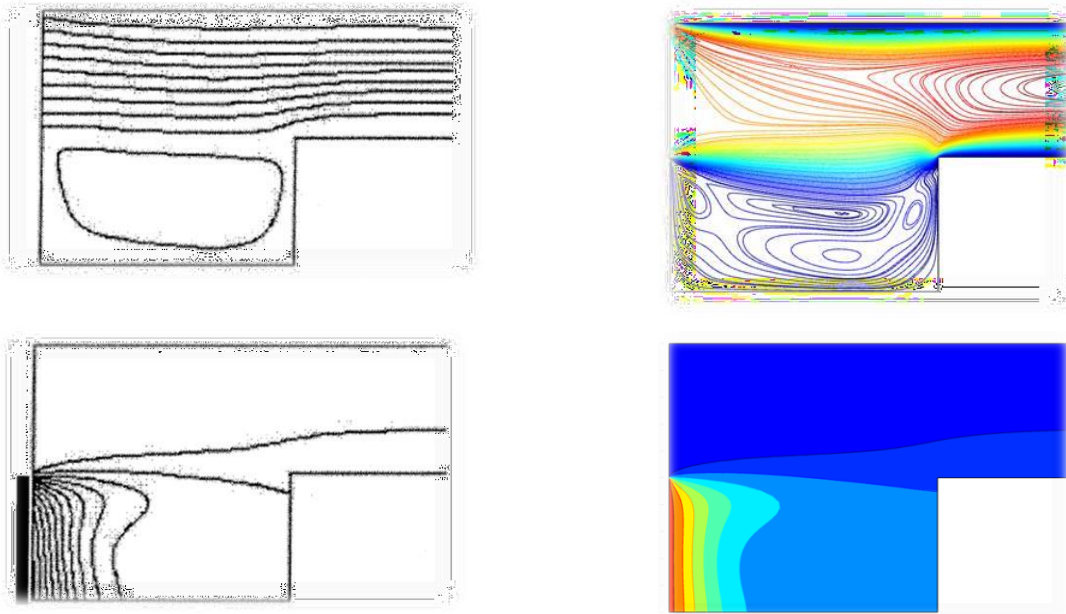


Figure 2. Comparison of streamlines and isotherms with the previous numerical study of Manca et al .[15].

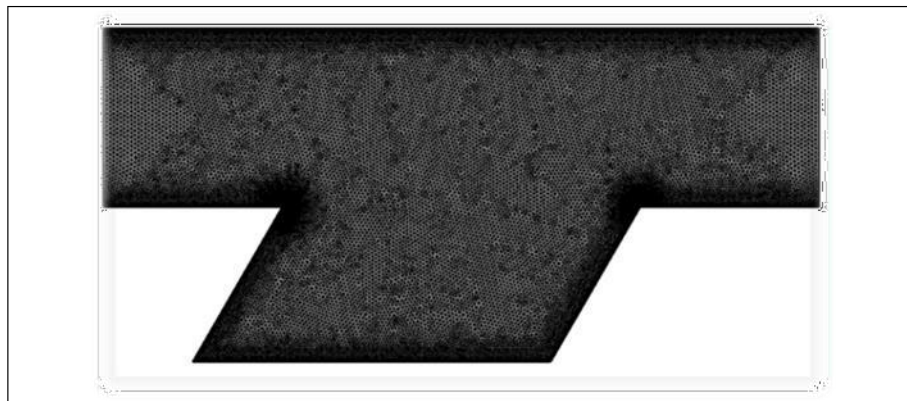


Figure 3. The generated grid G6 (44316 elements).

4. RESULTS AND DISCUSSION

Result are presented for 2D combined convection inside the channel with the cavity from streamline ,isotherm contour and the (Nu_{av}) and discussed for various value from Richardson number ($0.1 \leq Ri \leq 100$), for heat source length ϵ ($0.25 \leq \epsilon \leq 1$). At ($Re=100$) and ($Pr=0.71$).

4.1. Flow and thermal fields characteristic

4.1.1. Effect of the Richardson number(Ri)

The streamline and isotherm contours for assisting flow inside the channel-enclosure assembly for a different Richardson number ($0.1 \leq Ri \leq 100$) displayed in **Figs.(4 - 6)**. This effect was studied for ($0.25 \leq \epsilon \leq 1.0$) at ($Re=100$) .The variation in (Ri) has a clear effect on both the fields of the flow and thermal inside the cavity-channel assembly .Therefor ,the increase of it from ($Ri=0.1$) to ($Ri=100$) causes to a dramatic increase in flow disturbance inside the assembly .This can be evident from the growth of flow vortices and the increase in their numbers .This behaviour was repeated for all considered range in (ϵ) .Also ,the increase in (Ri) accelerates from the process of the thermal exchange inside the assembly and makes the air leaving process more fatly .The same positive effect of the increase in(Ri) can be seen on isotherm contours .So, the increase in it leads to increasethe cold regions inside the assembly as a signal a good flow mixing .Also, it increases the intensity of isotherms above the heat source compared with the case at low values of (Ri).

4.1.2. Effect of the length(ϵ) of the heat source

Figs.(4 - 6) illustrate also the effect of (ϵ) on the flow and thermal fields for assisting flow case. The result indicated that, the increase in (ϵ) from ($\epsilon=0.25$) to ($\epsilon=1.0$) does not effect on the flowfield pattern when the forced convection is dominant (i.e., $Ri=0.1$). While when the forced convection becomes equivalent to the natural convection forced or at ($Ri=1$), the increase in (ϵ) leads to construct a minor vortices adjacent the heat source. A clear change in the flow pattern in both the channel and cavity can be noted with the increase in (Ri), the effect of (ϵ) on the thermal fields. The results show that at ($Ri=0.1$), the increase in (ϵ) leads to extend the thermal plume far away from the heat source location towards the left sidewall leading to increase the hot regions inside the enclosure. But, at ($Ri=0.1$) the thermal plume begins to retard towards the heat source location and this retardation becomes more slow with the increase in (ϵ). Now, further increase in (Ri) causes the effect of (ϵ) restricts with the region above the location of the heat source. So, it can be noted from **Figs.(4-6)**, that the intensity of the thermal plume at this region increases with the increase in (ϵ) from ($\epsilon=0.25$) to ($\epsilon=1.0$). Therefore, it can be deduced that the increase in (ϵ) helps the thermal plume to leave more fast through the channel exit especially in the natural convection domain. Also, the increase in (ϵ) leads to increase the rate of the heat generation and increases the activity of the heat transfer by the natural convection due to the increase in the buoyancy force. An another word, the penetration of the flow to the cavity is increasing with the increase in (ϵ) consequently, the number of vortices is increasing and hence the heat transfer is increasing. The isotherms clearly show how the buoyancy force is increased with the increase of (ϵ), where clusters above the heat source are increasing and the shape of them turns to be vortices and hence the mixing of heat transfer in greatly increasing. Therefore, it can be concluded that the increase in (ϵ) has a positive contribution on the flow mixing between the channel and the enclosure especially at high value of (Ri).

4.1.3. Effect of the heat source location

Figs.(4-5) and **(7-8)** displays explain the influent of the location of the heat source on streamline and isotherm contours when it located at a same direction to the flow enters the channel. These figures are drawn at ($0.1 \leq Ri \leq 100$, $Re=100$ at $\epsilon=0.25$ and $\epsilon=0.75$). To illustrate this effect, a different location were considered. The first location, at the middle of the left sidewall of the cavity. While, the second location was assumed at the top corner of the same wall. The effect of the heat source location on the flow pattern, it can be seen that the change in it does not have a significant influence on the flow pattern when ($0.1 \leq Ri \leq 1$). This can be approved from the similar flow pattern in **Figs.(4)** and **(7)** for ($\epsilon=0.25$), **Figs.(5)** and **(8)** for ($\epsilon=0.75$) for this range of (Ri). But for the range ($10 \leq Ri \leq 100$), this difference between the flow fields becomes more explicit. Therefore, it can be concluded that the effect of the heat source location is more evident pronounced for the natural convection domain than the forced convection one. For the thermal field, the results show that the isotherms are clustered near the heat source location which indicates a high temperature gradient in this place. Also, it can be noted that the thermal plume can be seen when the heat source located at the center of the right wall of the enclosure especially at ($0.1 \leq Ri \leq 1$). While, it was absent for another considered location. Now, with the increase in (Ri) to ($10 \leq Ri \leq 100$), the effect of the heat source location begins to diminish gradually except in the region above the heat source. This can be indicated from the high similarity of the thermal fields in **Figs.(4)** and **(7)**, **(5)** and **(8)** at ($10 \leq Ri \leq 100$)

4.2. Heat transfer performance

4.2.1. Effect of the heat source length (ϵ) on average Nusselt number

Fig.(9) was described the variation in the average Nusselt number with (Ri) for various value of (ϵ) at ($Re=100$). The heat source location at a same direction to the flow enters the channel. In **Fig.(9)**, the heat source was located in the first location in the center of the left wall of the cavity, whereas the second location in upper region of the same wall. It can be seen for both location that, the values increase in (ϵ) and (Ri) increase the (Nu_{av}). For ($0.1 \leq Ri \leq 1.0$), the (Nu_{av}) varies linearly with (Ri), while a clear increase in it can be observed beyond this range of (Ri). This logical result confirms the dominance of the natural convection for high values on (Ri). This behaviour can be seen for all values of (ϵ) and both the location of the heat source.

4.2.2. Effect of the location of the heat source on the average Nusselt number.

Fig.(9) also explain the change location of the heat source on (Nu_{av}) values. By comparing the results presented in this figure. It can be seen that, the (Nu_{av}) was enhanced when the heat source was located in the upper region of the left wall. This increasing can be observed for all selected values of (ϵ). Since, in this location the cold fluid comes from the channel reaches the heat source fast than that when the heat source located in the middle of the left side wall. This location helps to distribute the hot air better than the another consider location and the

temperature difference between hot air and the cold air enters from the channel. Therefore, the temperature gradient between them increases and enhances the (Nu_{av}) values.

5. CONCLUSION

Combined convection in a parallelogram open cavity, fully and partially heated from the right sidewall of the enclosure has been studied numerically. The findings that follow can be deduced from the results of this work:

1. The heat transfer rate and flow circulation enhance by increasing in the heat source length the and (Ri)
2. The flow and thermal fields were significantly effect by the variation of (Ri) , the length and location of the heat source.
3. The Nu_{avg} was enhanced with increasing the (Ri) and (ϵ) .

The maximum values of Nu_{avg} is achieved for higher heat source length and in the upper region of the left wall of the cavity.

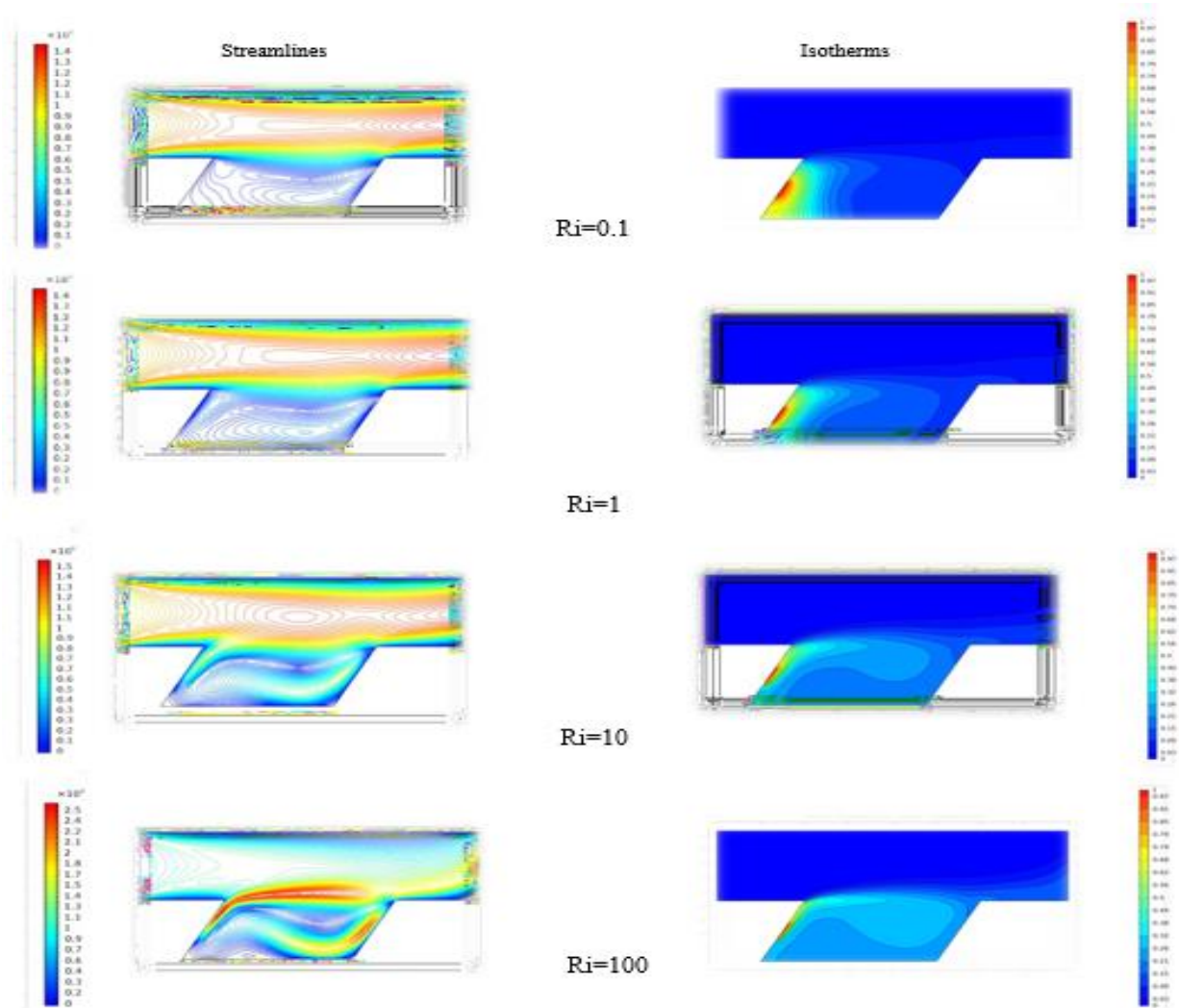


Figure 4. Streamlines and Isotherms for various values of the Richardson number of assisting flow belowat ($\epsilon=0.25$, $Re=100$) related to (The center of the left wall).

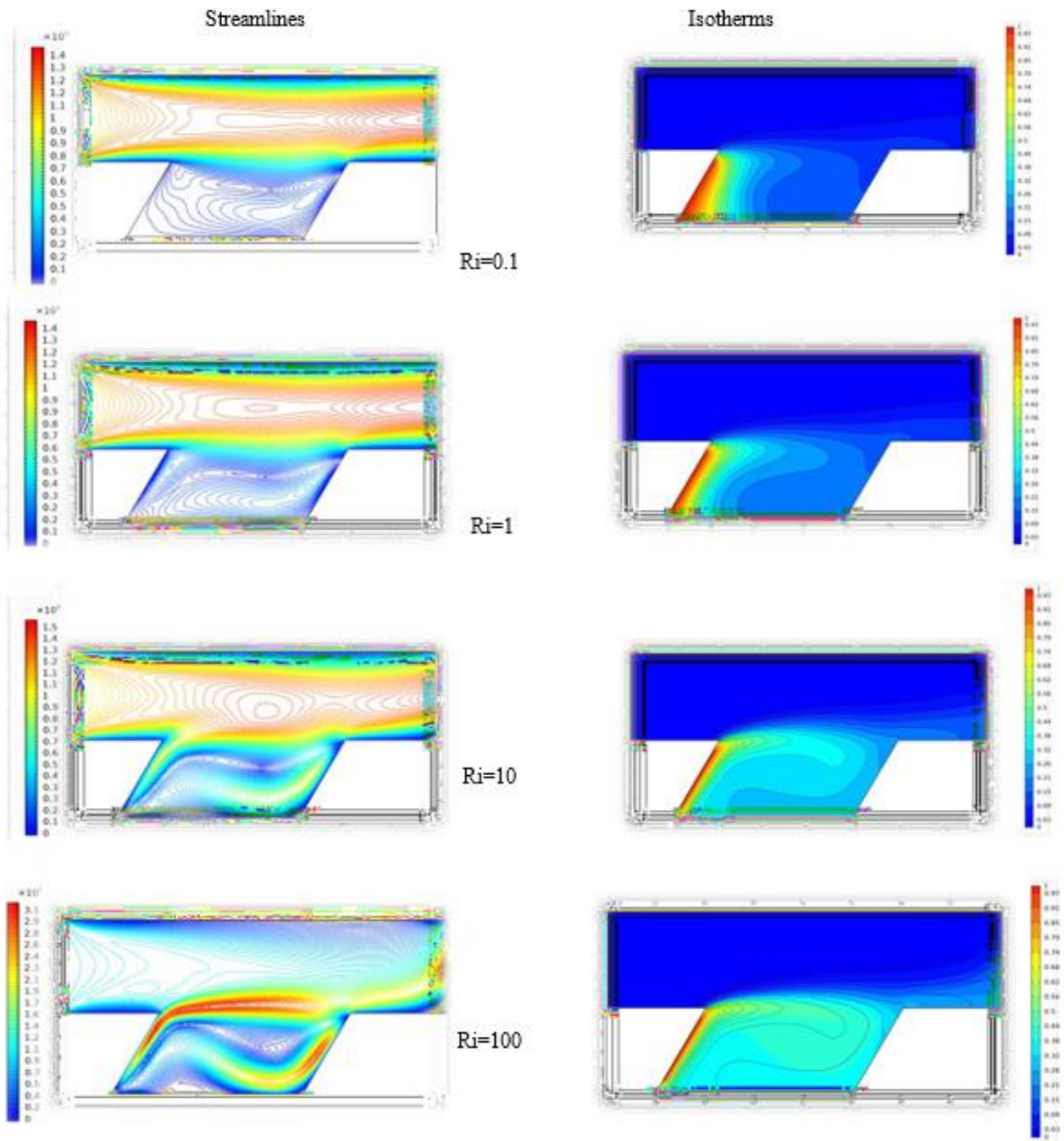


Figure 5. Streamlines and Isotherms for various values of the Richardson number of assisting flow at $\epsilon=0.75$, $Re=100$ (related to (The center of the left wall)).

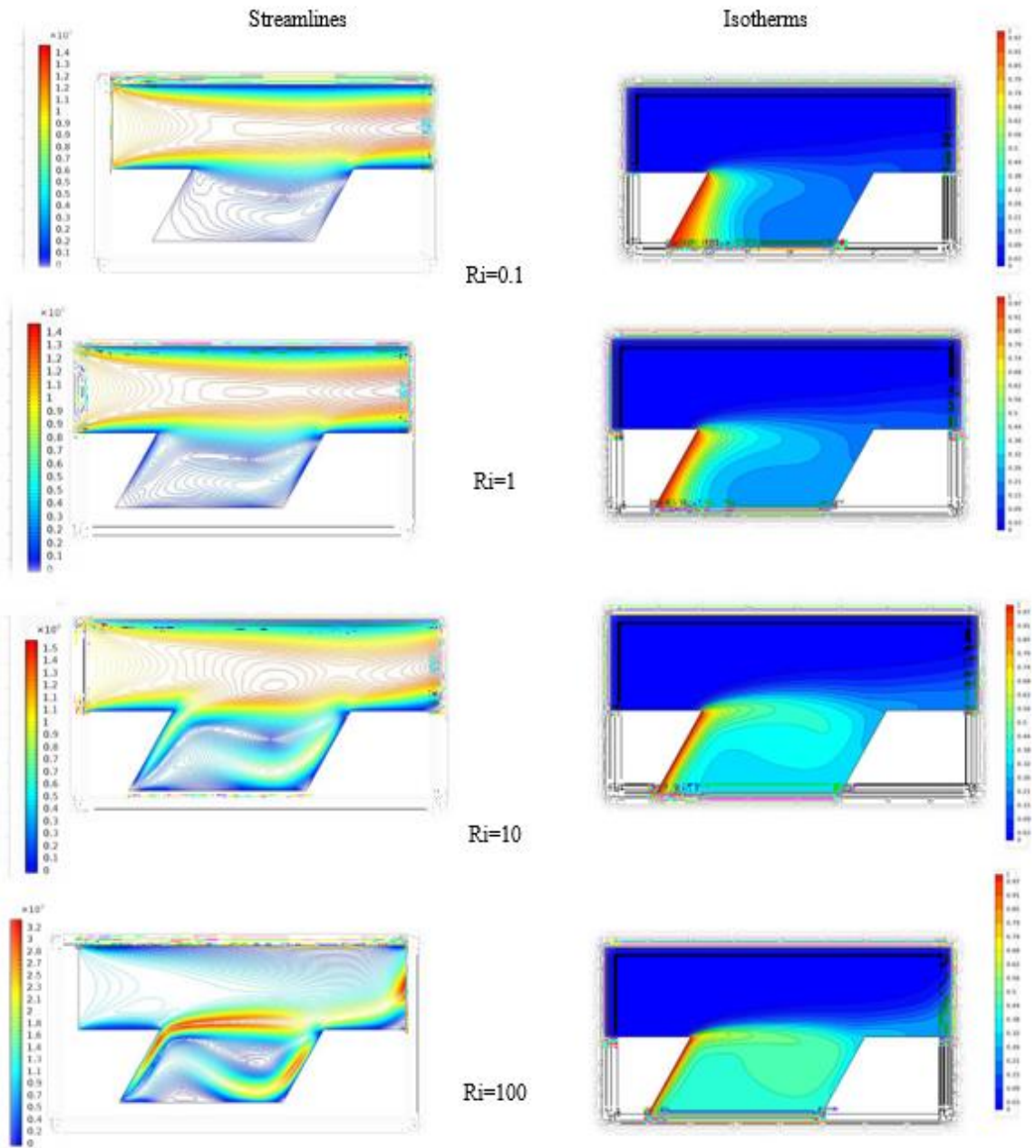


Figure 6. Streamlines and Isotherms for various values of the Richardson number of assisting flow at ($\epsilon=1, Re=100$).

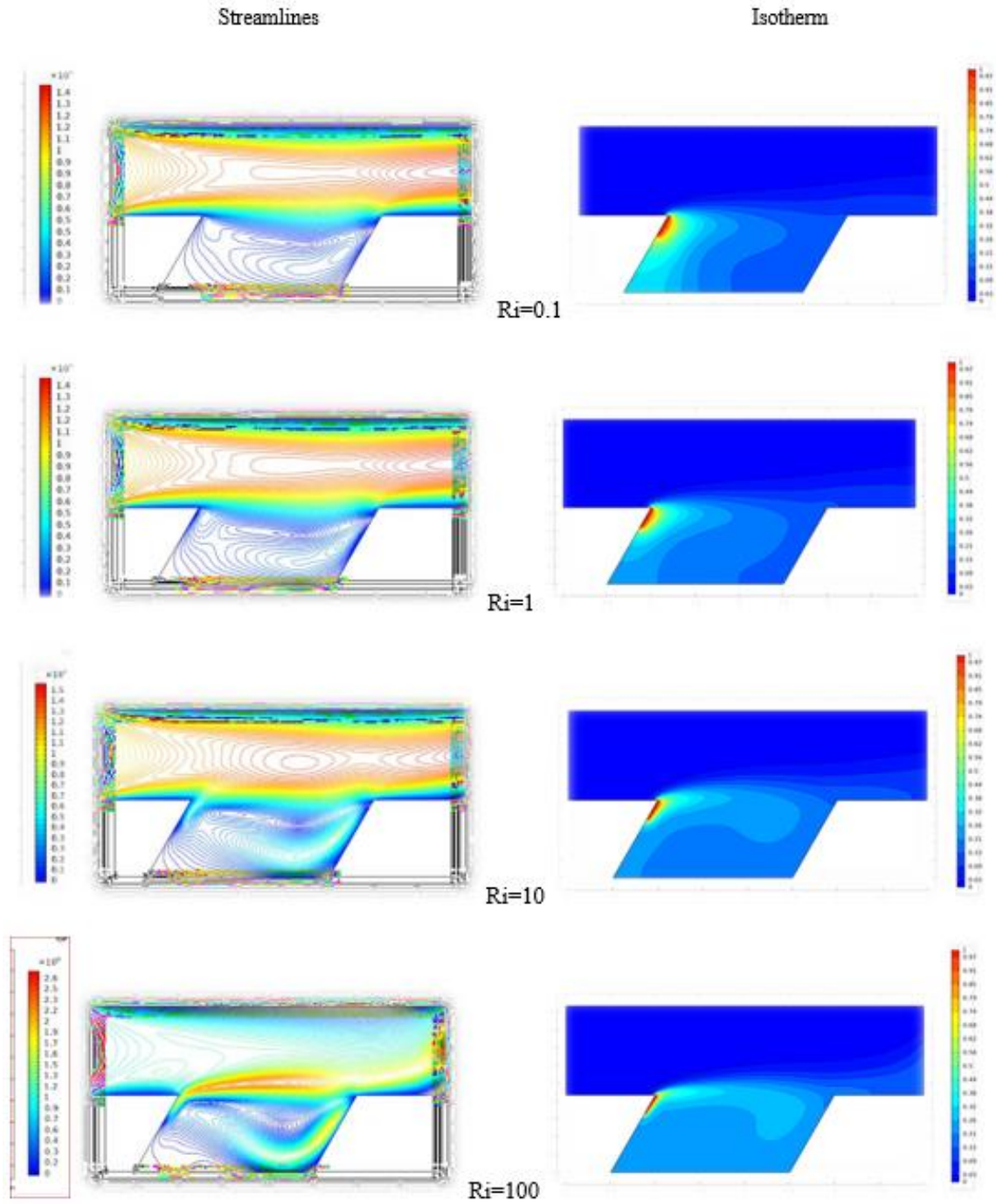


Figure 7. Streamlines and Isotherms for various values of the Richardson number of assisting flow at ($\epsilon=0.25$, $Re=100$) related to (The upper region of the left wall).

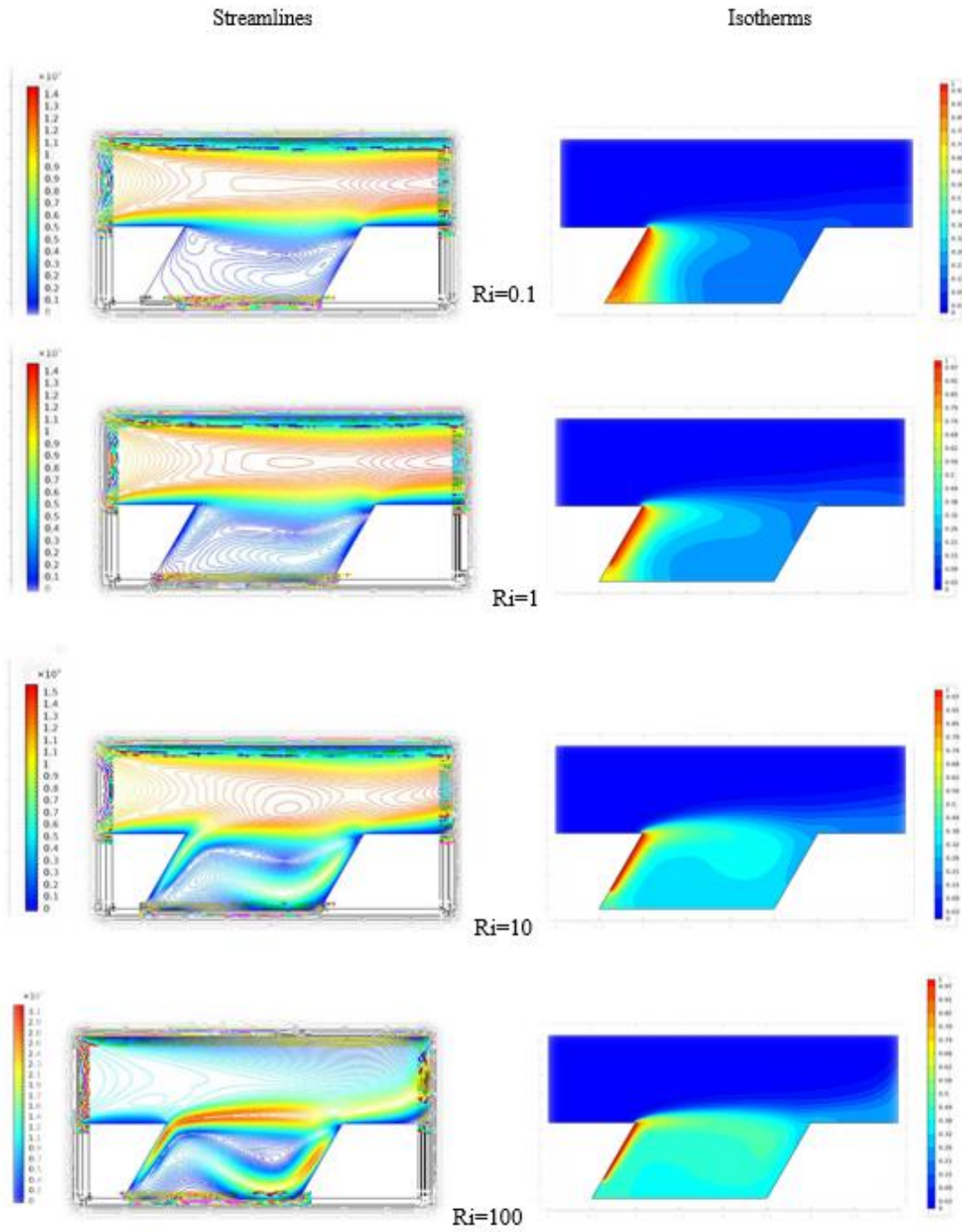


Figure 8. Streamlines and Isotherms for various values of the Richardson number of assisting flow at ($\epsilon=0.75$, $Re=100$) related to (The upper region of the left wall).

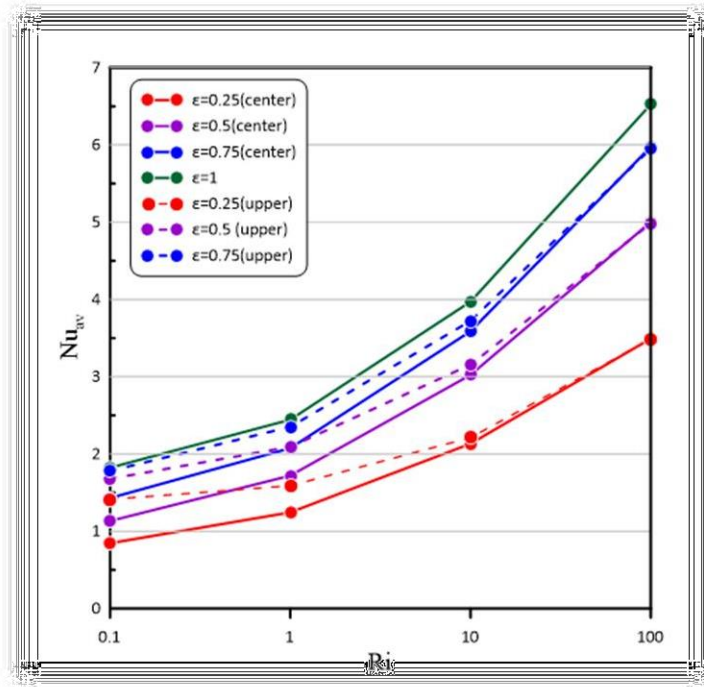


Figure 9. Variation of the average Nusselt number with the Richardson number for assisting flow.

Nomenclatures

D	height of the channel	(m)
g	gravitational acceleration	(m/s ²)
Gr	Grashof number	
H	height and the width of the cavity	(m)
Le	exit length	(m)
LH	Length of the localized heat source	(m)
n	normal vector	
Nu	Nusselt number	
p	pressure	(N/m ²)
P	dimensionless pressure	
Pr	Prandtl number	
Re	Reynolds number	
Rer	Reynolds numbers ratio	
Ri	Richardson number	
T	temperature	(°C)

u	velocity component in x-direction	(m/s)
U	dimensionless velocity component in X-direction	
v	velocity component in y-direction	(m/s)
V	dimensionless velocity component in Y-direction	
x	Cartesian coordinate in the horizontal direction	(m)
X	dimensionless coordinate in horizontal direction	
y	Cartesian coordinate in vertical direction	(m)
Y	dimensionless coordinate in vertical direction	

Greek Symbols

α	thermal diffusivity	(m ² /s)
β	thermal expansion coefficient	(1/K)
Θ	dimensionless temperature	
ϵ	Dimensionless length of the localized heat source	
μ	dynamic viscosity	kg/m s)
ν	kinematic viscosity	(m /s)
ρ	density	(kg/m ³)
Φ	angle of the cavity sidewalls	(deg)
ψ	stream function	(m /s)
Ψ	dimensionless stream function	

Subscripts

av	average
c	cold
h	Hot
in	Inlet

REFERENCES

1. Hussain, S. and Hussein, A.K. Mixed convection heat transfer in a differentially heated square enclosure with a conductive rotating circular cylinder at different vertical locations , International Communications in Heat and Mass Transfer, Vol.38, 2011, pp : 263-274.
2. Sivasankaran ,S., Sivakumar ,V., Hussein ,A.K, and Prakash ,P. Mixed convection in a lid-driven two- dimensional square cavity with corner heating and internal heat generation. Nume Heat Transfer -Part A. Vol .65,No.3 ,2014 , pp :269-286.
3. Hussein, A.K. and Hussain, S.Characteristics of magneto-hydrodynamic mixed convection in a parallel motion two-sided lid- driven differentially heated parallelogrammic cavity with various skew angles, Journal of Thermal Engineering, Vol. 1, No. 3, 2015, pp. 221-235.
4. Hussein, A.K. Entropy generation due to the transient mixed convection in a three- dimensional right-angle triangular cavity, International Journal of Mechanical Sciences, Vol.146-147, 2018, pp : 141-151.
5. Mallikarjuna, B., Rashad, A., Hussein, A.K. and Raju, S. Transpiration and thermophoresis effects on non- Darcy convective flow past a rotating cone with thermal radiation, Arabian Journal for Science and Engineering, Vol. 41, No.11, 2016, pp : 4691- 4700.
6. Mohammed, H., Al-Aswadi, A., Abu-Mulaweh, H., Hussein, A.K. and Kanna, P. Mixed convection over a backward-facing step in a vertical duct using nanofluids-buoyancy opposing case, Journal of Computational and Theoretical Nanoscience, Vol.11, 2014, pp : 1-13.

7. Ahmed, S., Mansour, M., Hussein, A.K and Sivasankaran, S. Mixed convection from a discrete heat source in enclosures with two adjacent moving walls and filled with micropolar nanofluids, *Engineering Science and Technology - an International Journal*, Vol.19, No.1, 2016, pp : 364-376.
8. Saha, S., Hussein, A.K., Saha, G. and Hussain, S. Mixed convection in a tilted lid-driven square enclosure with adiabatic cylinder at the center, *International Journal of Heat and Technology*, Vol. 29, No. 1, 2011, pp. 143- 156.
9. Al-Rashed, A., Kalidasan, K., Kolsi, L., Velkennedy, R., Aydi, A., Hussein, A.K. and Malekshah ,E. Mixed convection and entropy generation in a nanofluid filled cubical open cavity with a central isothermal block, *International Journal of Mechanical Sciences*, Vol. 135, 2018, pp : 362-375.
10. Mebarek-Oudina . F. and Bessaïh, R. Numerical Simulation of Natural Convection Heat Transfer of Copper- Water Nanofluid in a Vertical Cylindrical Annulus with Heat Sources, *Thermophysics and Aeromechanics*, Vol. 26, No. 3, 2019, pp : 325-334.
11. Mebarek-Oudina , F, Convective Heat Transfer of Titania Nanofluids of different base fluids in Cylindrical Annulus with discrete Heat Source, *Heat Transfer-Asian Research*, Vol. 48, No.1, 2019, pp: 135-147.
12. Gourari, S., Mebarek-Oudina, F., Hussein, A.K., Kolsi , L. , Hassen , W. and Younis , O. Numerical study of natural convection between two coaxial inclined cylinders, *International Journal of Heat and Technology*, Vol. 37, No. 3, 2019 , pp. 779-786.
13. Selimefendgil ,F. and Öztop ,HF. Numerical study and identification of cooling of heated blocks in pulsating channel flow with a rotating cylinder, *International Journal of Thermal Sciences* , Vol.79,2014, pp:132-145.
14. Manca, O., Nardini, S., Khanafer, K. and Vafai, K. Effect of heated wall position on mixed convection in a channel with an open cavity, *Numerical Heat Transfer - Part A*, Vol. 43, No. 3, 2003, pp : 259-282.
15. Manca O., Nardini ,S. and Vafai ,K. Experimental investigation of mixed convection in a channel with an open cavity. *Experimental Heat Transfer*, Vol.19, No. 1, 2006, pp:53-62.
16. Leong, J., Brown, N. and Lai, F. Mixed convection from an open cavity in a horizontal channel , *International Communications in Heat and Mass Transfer*, Vol. 32, 2005 , pp : 583-592.
17. Aminossadati, S. and Ghasemi, B. A numerical study of mixed convection in a horizontal channel with a discrete heat source in an open cavity, *European Journal of Mechanics B/Fluids*, Vol. 28, 2009, pp : 590-598.
18. Rahman, M., Parvin, S., Saidur, R. and Rahim, N. Magnetohydrodynamic mixed convection in a horizontal channel with an open cavity, *International Communications in Heat and Mass Transfer*, Vol.38, 2011, pp : 184-193.
19. Rahman, M., Parvin S., Rahim, N., Hasanuzzaman , M. and Saidur , R. Simulation of mixed convection heat transfer in a horizontal channel with an open cavity containing a heated hollow cylinder , *Heat transfer – Asianresearch*, Vol.41, No.4 , 2012, pp : 339-353.
20. Carozza ,A., Manca ,O. and Nardini ,S . Numerical Investigation on Heat Transfer Enhancement due to Assisting and Opposing Mixed Convection in an Open Ended Cavity, 2nd International Conference on Emerging Trends in Engineering and Technology London (UK) May 30-31, 2014 (ICETET'2014), pp : 85-90.
21. Laouira, H., Mebarek-Oudina, F., Hussein, A.K. , Kolsi, L., Merah, A. and Younis, O. Heat transfer inside a horizontal channel with an open trapezoidal enclosure subjected to a heat source of different lengths, *Heat Transfer-Asian Research*, Vol.49, 2020, pp: 406-423.
22. Mebarek- Oudina F ., Laouira H , Aissa , Hussein ,A. K. and El Ganaoui M. Convection Heat Transfer Analysis in a Channel with an Open Trapezoidal Cavity: Heat Source Locations effect MATEC Web of Conferences 330, 01006 (2020), pp:1-5.
23. AL-Farhany , K., Azeez Alomari1, M., and Faisa, A. Magnetohydrodynamics Mixed Convection Effects on the open enclosure in a horizontal channel Heated Partially from the Bottom, *IOP Conf. Series: Materials Science and Engineering* 870, 012174 (2020) ,pp:1-7
24. Manca ,O., Nardini ,S. and Vafai ,K. Experimental investigation of opposing mixed convection in a channel with an open cavity below. *Experimental Heat Transfer*, Vol.21, No.2, 2008. Pp:99-114.
25. Stiriba, Y. Analysis of the flow and heat transfer characteristics for assisting incompressible laminar flow past an open cavity , *International Communications in Heat and Mass Transfer*, Vol. 35, 2008, pp : 901-907.
26. Burgos, J., Cuesta, I. and Saluena, C. Numerical study of laminar mixed convection in a square open cavity , *International Journal of Heat and Mass Transfer*, Vol. 99, 2016, pp : 599-612
27. Sabbar W A., Ismae M. A. , Almudhaffar M. Fluid-structure interaction of mixed convection in a cavity- channel assembly of flexible wall, *International Journal of Mechanical Sciences* ,Vol .149, 2018, PP:73–83
28. Yasin, N., Jehhef, K. and Shaker, A. Assessment of the baffle effects on the mixed convection in open cavity, *International Journal of Mechanical and Mechatronics Engineering*, Vol.18, No.4, 2018, pp : 1-14.
29. Cardenas, V., Trevino, C., Rosas, I. and Martinez-Suastegui, L., Experimental study of buoyancy and inclination effects on transient mixed convection heat transfer in a channel with two symmetric open cubic cavities with prescribed heat flux, *International Journal of Thermal Sciences*, Vol. 140, 2019, pp : 71-86.
30. Contreras, H., Trevino, C., Lizardi, J. and Martinez-Suastegui, L., Stereoscopic TR-PIV measurements of mixed convection flow in a vertical channel with an open cavity with discrete heating, *International Journal of Mechanical Sciences*, Vol. 150, 2019, pp : 427-444.
31. Altaca Z and Timuralp C . Investigation of fluid flow and heat transfer in a channel with an open cavity heated from bottom side .*Mugla Journal of Science and Technology*, Vol 2, No .1, 2016, pp:55-59
32. Rahman, M., Oztot, H., Rahim, N., Saidur, R., Al-Salem, K., Amin, N., Mamun, M. and Ahsan, A. Computational analysis of mixed convection in a channel with a cavity heated from different sides, *International Communications in Heat and Mass Transfer*, Vol. 39, 2012, pp : 78-84.
33. Abdelmassih, G., Vernet, A. and Pallares, J. Steady and unsteady mixed convection flow in a cubical open cavity with the bottom wall heated , *International Journal of Heat and Mass Transfer*, Vol. 101, 2016, pp : 682-691.

- 34.** Garcia, F., Trevino, C., Lizardi, J. and Martinez-Suastegui, L. Numerical study of buoyancy and inclination effects on transient mixed convection in a channel with two facing cavities with discrete heating, *International Journal of Mechanical Sciences*, Vol. 155, 2019, pp : 295-314.
- 35.** Ismael , M. A., Hussein, A. K., Mebarek-Oudina, F. and Kolsi, L. Effect of Driven Sidewallson Mixed Convection in an Open Trapezoidal Cavity With a Channel, *Journal of Heat Transfer*, Vol .142 ,2020, pp :082601-1

DOI: <https://doi.org/10.15379/ijmst.v10i2.1422>

This is an open access article licensed under the terms of the Creative Commons Attribution Non-Commercial License (<http://creativecommons.org/licenses/by-nc/3.0/>), which permits unrestricted, non-commercial use, distribution and reproduction in any medium, provided the work is properly cited.